CYCLIC PLASTIC RESPONSE AND FATIGUE LIFE OF DUPLEX AND SUPERDUPLEX STAINLESS STEELS

JAROSLAV POLÁK

Institute of Physics of Materials, Academy of Sciences of the Czech Republic, Žižkova 22, 616 62 Brno, Czech Republic

Received 31 January 2005, accepted 22 February 2005

Two austenitic-ferritic duplex steels with different nitrogen content were subjected to cyclic loading in a wide interval of fatigue lives with controlled plastic strain amplitude and controlled stress amplitude. Cyclic hardening/softening curves, cyclic stress-strain curves and fatigue life curves were measured and parameters of individual curves were evaluated. Both types of loading result in nearly identical cyclic stress-strain curves and fatigue life curves. Cyclic stress-strain curve and Wöhler curve of a superduplex steel are higher than those of duplex steel but Manson-Coffin curves of both steels are identical. The experimental data and evaluated parameters characterize the fatigue resistance of both advanced materials in a wide interval of fatigue lives.

K e y w o r d s: duplex steel, fatigue life, cyclic plasticity, plastic strain amplitude

1. Introduction

Duplex stainless steels are two-phase austenitic-ferritic alloys with principal alloying elements chromium, nickel and molybdenum. Their mechanical properties are often enhanced through nitrogen alloying. Nitrogen alloyed duplex stainless steels are very promising in terms of the combination of high strength and excellent corrosion resistance. Modern production metallurgy processes resulted in a series of products widely used in offshore industry, shipbuilding, petrochemical, oil and gas industry, pulp and paper industry and recently also in production of mechanical and structural components [1, 2]. The manufactured products are subjected to external forces of variable character or to repeated deformations due to temperature variations. Several studies of fatigue properties of individual duplex steels were performed in the past concentrating on low cycle fatigue [3–8] and fatigue crack

e-mail: polak@ipm.cz

growth [7, 9]. Effect of phase morphology [8] and geometrical arrangement of two phases and their crystallographic texture on the fatigue life [10] were studied. The cyclic plastic response has been studied in a limited way, mostly in low cycle domain [4, 6, 7].

In the wide interval of fatigue lives, fatigue life has been only reported by Akdut [8] for duplex steels with elevated nitrogen content. Considerable uncertainty exists in the cyclic stress-strain curves and no data are available on the hardening/softening behaviour in the high cycle domain.

We have therefore undertaken the complex study of the cyclic plastic behaviour and fatigue life in a wide interval of plastic strain amplitudes of two stainless duplex steels, i.e. the widely used 2205 duplex steel and 2207 superduplex steel utilized in most demanding applications. Both plastic strain amplitude controlled tests and stress amplitude controlled tests were performed.

2. Experiments

Austenitic-ferritic duplex stainless steels EN No. 1.4462 (Sandvik SAF 2205) and superduplex EN No. 1.4410 (Sandvik SAF 2507) were supplied by Sandvik, Sweden as rods of 70 mm and 30 mm in diameter, respectively. The chemical composition (in wt.%) was: 0.016 C, 22.0 Cr, 5.4 Ni, 3.1 Mo, 0.16 N, the rest Fe for SAF 2205 and 0.020 C, 23.0 Cr, 7.0 Ni, 3.8 Mo and 0.27 N, the rest Fe for SAF 2507. The structure of both steels was formed by islands of austenite elongated in the rolling direction, which were embedded in a ferritic matrix. Figure 1 shows the

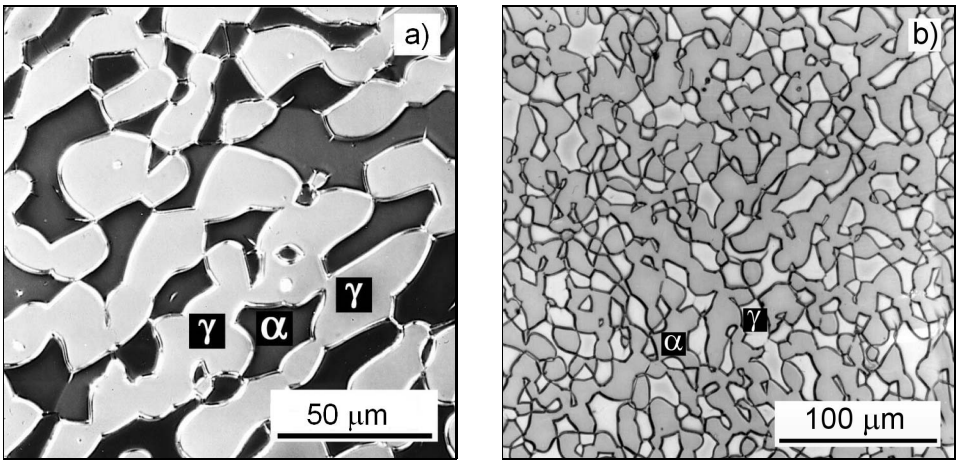

Fig. 1. Optical micrograph of a cross section (perpendicular to the specimen axis) of the SAF 2205 steel (a) and SAF 2507 steel (b) in polarized light.

optical micrograph in polarized light of the etched surface of both steels in sections perpendicular to the axis of the bar. The volume fraction of austenite is 46 % in SAF 2205 steel and 34 % in SAF 2507 steel.

Cylindrical specimens of the diameter 8 mm and of the gauge length 12 mm were manufactured and grinded in the central part to achieve a smooth surface. Specimens were cycled in MTS 880 computer controlled testing machine. The strain was measured and/or controlled with a longitudinal extensometer at the gauge length of 12 mm. In constant plastic strain amplitude loading symmetrical strain cycle was applied to the specimens. Strain rate 2.5×10^{-3} s^{-1} was held constant at the start of the cycling. The hysteresis loops were digitally recorded during the tests and the stress amplitude and the width of the hysteresis loop was stored. The plastic strain amplitude was evaluated from the half-width of the hysteresis loop in real time. The outer closed loop control was used to adjust the total strain amplitude in such a way that the plastic strain amplitude was kept constant. In order to prevent the overshoot of the plastic strain amplitude for very small plastic strain amplitudes at the start of cycling, the initial strain amplitude was fixed to a slightly lower level than expected and the computer algorithm resulted in approaching the desired level in 5 up to 30 initial cycles.

For higher plastic strain amplitudes, resulting in the fatigue lives below 10^4 cycles, the strain rate was held constant during the test. In order to achieve high number of cycles in a reasonable time for low plastic strain amplitudes, the loading regime has been modified in such a way that above 10^4 cycles instead of constant strain rate cycling the sinusoidal cycling with the same total strain amplitude, as determined in the last measurement of the hysteresis loop, and the frequency around 5 cycles s^{-1} was applied. Since the initial hardening/softening for all amplitudes has terminated before 10^4 cycles, the plastic strain amplitude could be kept constant also during each block of sinusoidal cycling. The constant strain rate loading was restored always for 20 cycles before the recording of the hysteresis loop. The hysteresis loop in sinusoidal cycling was also checked on the digital scope and was compared with that recorded in low strain rate cycling. The loops were nearly identical, which shows that the increase of the frequency and the change of the cycle shape had not a substantial effect on the size and the shape of the loop. This loading regime and the control of the grip temperature allowed keeping constant specimen temperature during cycling at all plastic strain amplitudes.

Analogous procedure was applied in constant stress amplitude loading. The loading cycle was sinusoidal with the initial stress rate equal to the applied strain rate in constant plastic strain amplitude cycling. Again, for the lowest stress amplitudes resulting in fatigue lives higher than 10^4 cycles the cycling frequency was intermittently increased to around 5 cycles s^{-1}. Twenty cycles before the recording of the hysteresis loop the initial frequency was restored.

During measurement of each hysteresis loop the effective modulus in tensile

unloading was evaluated and compared with that measured at 500 cycles. Due to the appearance of the principal crack in the gauge length the effective modulus started to decrease. The number of cycles to fracture, N_f, was determined when the effective modulus in tensile unloading dropped to 90 % of the value measured at 500 cycles. This drop of the effective modulus in tensile unloading corresponds to the appearance of a macroscopic crack of the surface length about 2 mm. The cycling continued until the principal crack extended to nearly whole cross section, which corresponded to the drop of the effective modulus in tensile unloading to around 50 % of the value measured at 500 cycles. The corresponding additional number of cycles represented only negligible fraction of N_f. It increased with the plastic strain amplitude similarly as N_f but had higher scatter than N_f.

3. Results

Both SAF 2205 and SAF 2507 steels were subjected to constant plastic strain amplitude loading with plastic strain amplitudes in the interval from 2×10^{-5} to 1×10^{-2}. Figure 2 shows the cyclic hardening-softening curves in constant plastic strain amplitude regime. Behaviour of both steels is similar; i.e. initial hardening at high plastic strain amplitudes is followed by softening and saturation. Due to slow adjustment of the plastic strain amplitude at low amplitudes (up to the dot--and-dash line in Fig. 2) the initial hardening/softening behaviour could not be documented. In low plastic strain amplitude cycling slight softening is followed by stabilized stress amplitude. A tendency to long-term cyclic hardening in low plastic strain amplitude cycling is observed for both steels.

SAF 2507 steel was also cycled in constant stress amplitude cycling. Figure 3 shows plastic strain amplitude vs. number of cycles. Cyclic softening follows rapid initial hardening for all stress amplitudes. For high stress amplitudes cyclic softening continues until fracture, for low stress amplitudes plastic strain amplitude saturates and in long-term cycling even the cyclic hardening is observed.

Cyclic stress-strain curves were plotted as the dependence of the stress amplitude at half-life vs. the applied plastic strain amplitude or as the applied stress amplitude vs. the plastic strain amplitude at half-life. For the lowest plastic strain amplitudes or the lowest stress amplitudes for which the specimen did not fracture, the stress and plastic strain amplitudes of the last recorded hysteresis loop were used in plotting the cyclic stress-strain curve. Figure 4 shows cyclic stress-strain curves for both steels as obtained from constant plastic strain amplitude cycling. The parameters K and n of the power law

$$\sigma_a = K\varepsilon_{ap}^n \tag{1}$$

fitted to both sets of data using least squares method are shown in Table 1. The data from constant plastic strain amplitude cycling and from constant stress amplitude

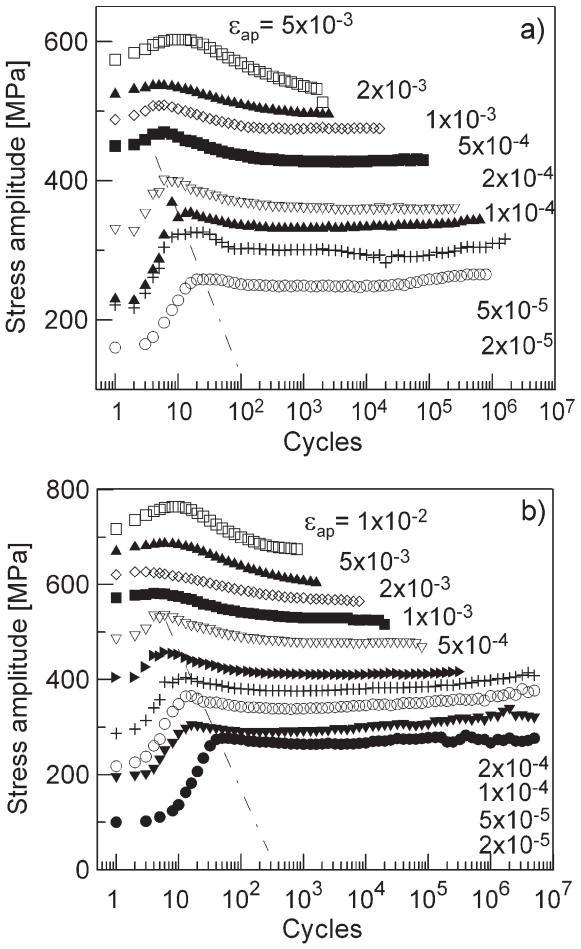

Fig. 2. Fatigue hardening/softening curves in constant plastic strain amplitude loading: a) SAF 2205 steel, b) SAF 2507 steel.

cycling for SAF 2507 steel are shown in Fig. 5. It is apparent that both types of cycling result in an identical stress-strain curve. The parameters of the power law (1) fitted separately to both sets of data (corresponding straight lines are plotted in Fig. 5) differ negligibly.

Manson-Coffin curves of both steels derived from constant plastic strain amplitude cycling are shown in Fig. 6. Both curves differ only slightly. The parameters $\varepsilon'_{\mathrm{f}}$ and c of the Manson-Coffin law

$$\varepsilon_{\mathrm{ap}} = \varepsilon'_{\mathrm{f}} \, (2N_{\mathrm{f}})^{c} \tag{2}$$

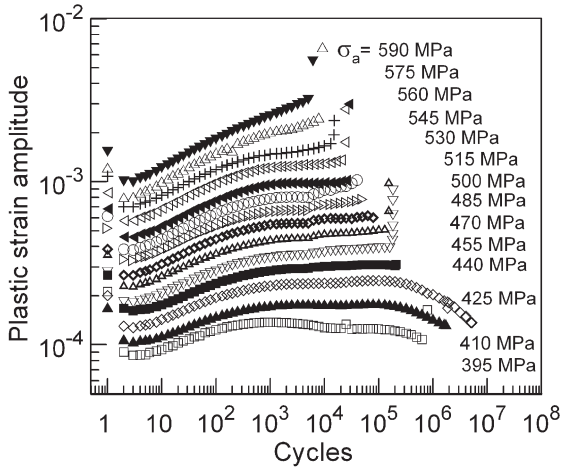

Fig. 3. Fatigue hardening/softening curves in stress amplitude loading; SAF 2507 steel.

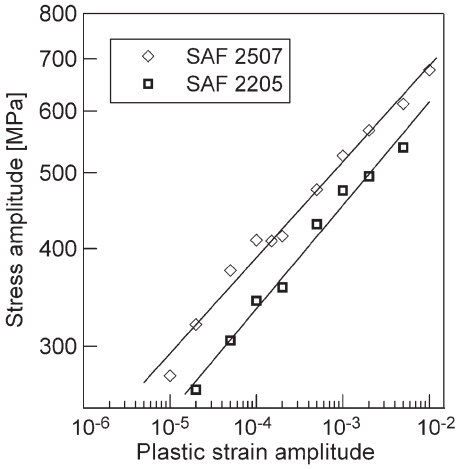

Fig. 4. Cyclic stress-strain curves of two duplex steels.

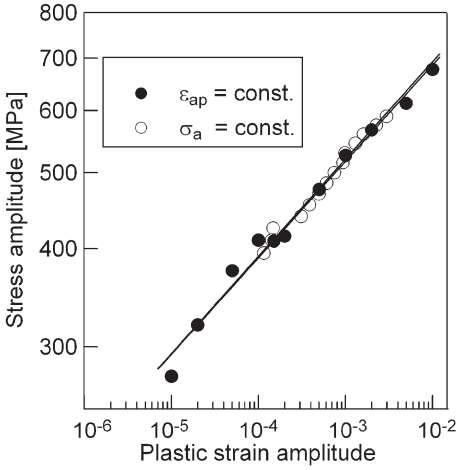

Fig. 5. Cyclic stress-strain curve of SAF 2507 steel from constant plastic strain amplitude and constant stress amplitude testing.

were fitted to the data corresponding to finite lives of both steels and are shown in Table 1.

Table 1. Parameters of the cyclic stress-strain curves and fatigue life curves of two duplex steels

Material	K [MPa]	n	$\varepsilon'_{\mathrm{f}}$	c	σ'_{f}	b
SAF 2205	1133	0.132	0.831	−0.627	1042	−0.0774
SAF 2507	1208	0.123	0.745	−0.600	1144	−0.0726

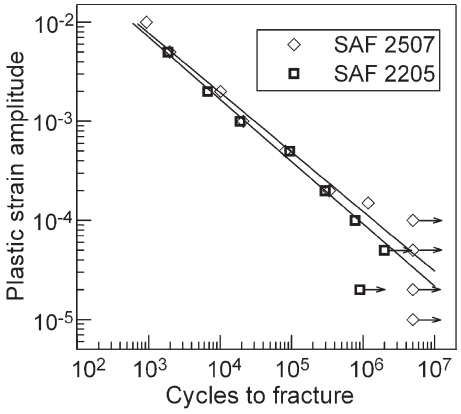

Fig. 6. Manson-Coffin curves of two duplex steels.

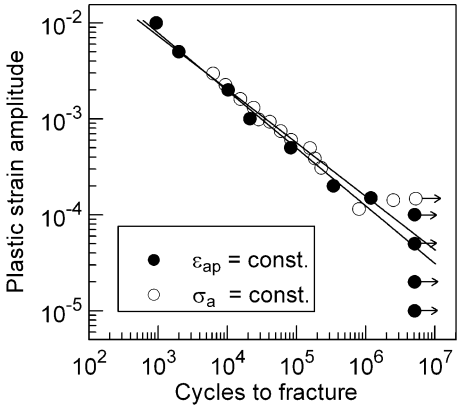

Fig. 7. Manson-Coffin curve of SAF 2507 steel from constant plastic strain amplitude and constant stress amplitude testing.

Manson-Coffin plots obtained from constant plastic strain amplitude tests and constant stress amplitude tests of SAF 2507 steel are shown in Fig. 7. Very good agreement between both sets of data is obtained and also the power laws (2) fitted to each set of data are very close.

Derived Wöhler curves from constant plastic strain amplitude cyclic loading of both steels are shown in Fig. 8. Both curves can be very well approximated by the Basquin law

$$\sigma_{\mathrm{a}} = \sigma'_{\mathrm{f}} \left(2N_{\mathrm{f}}\right)^{b} . \tag{3}$$

The parameters σ'_{f} and b were evaluated using least square fit and are shown in Table 1. Due to the higher stress response of the SAF 2507 steel (see Fig. 4) the derived Wöhler curve of this steel is above that of SAF 2205 steel.

Figure 9 shows Wöhler curve (obtained from constant stress amplitude tests) and derived Wöhler curve (obtained from constant plastic strain amplitude tests) of the SAF 2507 steel in a single plot. Very good agreement between the results of both testing procedures is obtained. The parameters σ'_{f} and b of both curves were

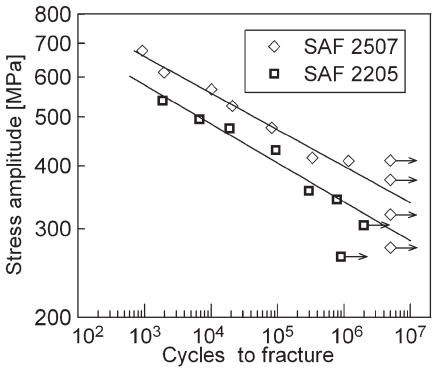

Fig. 8. Derived Wöhler curves of two duplex steels.

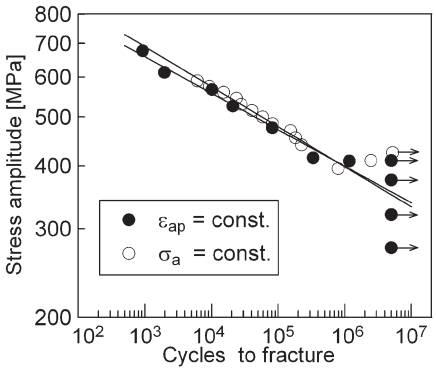

Fig. 9. Wöhler curve from constant stress amplitude testing and derived Wöhler curve from constant plastic strain amplitude testing of SAF 2507 steel.

evaluated but since they differ only slightly only the parameters of the derived Wöhler curve are shown in Table 1.

4. Discussion

Fatigue hardening/softening curves of both steels measured in constant plastic strain amplitude regime show only small variations of the stress amplitude during the fatigue life. For the lowest plastic strain amplitudes stabilized behaviour with a tendency to long-term cyclic hardening is observed. The long-term softening follows the initial hardening for the highest plastic strain amplitudes (see Fig. 2). Stabilized behaviour is observed for medium strain amplitudes. The changes of the cyclic stress-strain response are more pronounced in constant stress amplitude cycling shown for SAF 2507 steel in Fig. 3. For the highest stress amplitudes the logarithm of the plastic strain amplitude is proportional to the logarithm of the number of cycles. At medium stress amplitudes the softening is followed by stabilized behaviour. For the lowest stress amplitudes and high number of cycles the material starts to harden again. The long-term hardening is most probably the reason why specimens cycled with the lowest stress amplitude did not fracture provided no macroscopic defect was present on the specimen surface. The data for SAF 2507 steel show that cyclic hardening/softening behaviour of this material is equivalent in plastic strain and in stress controlled cycling.

The comparison of cyclic stress-strain curves determined from constant stress amplitude cycling and constant plastic strain amplitude cycling (Fig. 5 and Table 1) shows excellent agreement. The stress amplitude at half-life was plotted vs. applied

plastic strain amplitude in plastic strain-controlled tests and applied stress amplitude was plotted vs. the plastic strain amplitude at half-life for stress-controlled tests. Cyclic stress response of the SAF 2507 steel is higher (around 70 MPa) than that of SAF 2205 steel (Fig. 4) in the whole interval of plastic strain amplitudes. This is in agreement with the data in low cycle fatigue domain [4].

Most important data represent the fatigue life curves (Figs. 6 to 9). Figures 7 and 9 demonstrate clearly for SAF 2507 steel that if the experiments are performed with a very good control of the stress amplitude and/or plastic strain amplitude both Manson-Coffin curves (Fig. 7) and Wöhler curves (Fig. 9) evaluated from two extreme types of cyclic loading (constant stress amplitudes and constant plastic strain amplitudes) are identical.

Manson-Coffin curves of both steels (Fig. 6 and Table 1) are very close each other. Single power law of the type (2) can be fitted to both sets of experimental data up to number of cycles 5×10^6. Several specimens, both in stress-controlled and in strain-controlled regimes, did not fracture until 5×10^6 cycles. The plastic strain amplitude, which corresponds to the life higher than 5×10^6 cycles, can be read from the Manson-Coffin curve and corresponds to 1×10^{-4}. It is the plastic strain fatigue limit (at the conventional fatigue limit 5×10^6 cycles). It is high in both steels and witnesses about the high resistance of the austenitic-ferritic duplex structure to the initiation and growth of fatigue cracks [11].

The present results can be compared with the measurements of Akdut [8], who published Manson-Coffin curves of fine and gross grained wrought A905 duplex steel simultaneously with that of cast 2205 duplex steel down to fatigue life of 10^6 cycle. All his specimens fractured. Akdut did not evaluate the parameters of the Manson-Coffin law but our evaluation of his data yields parameters very close to the parameters assessed for both duplex steels studied in this work (see Table 1). Apparent disagreement Akdut's and also our results with the earlier results of Degallaix et al. [4] in low cycle fatigue domain (see Fig. 8 in Akdut's paper [8]) is due to an error in Akdut's paper when plotting Fig. 8 caused by substitution of plastic stress range for plastic strain amplitude (factor of 2).

5. Conclusions

Most important conclusions of this work can be summarized as follows:

(i) Cyclic stress-strain response of SAF 2507 duplex in constant plastic strain amplitude testing and constant stress amplitude testing is similar. The cyclic stress--strain curve, the Manson-Coffin curve and the derived Wöhler curve obtained from both loading regimes are identical.

(ii) Power law type laws describe the fatigue life curves and cyclic stress-strain curves in a wide amplitude interval comprising low and high cycle fatigue.

(iii) High limiting plastic strain amplitude (1×10^{-4}) at the conventional fatigue limit (5×10^6 cycles) was obtained witnessing the high resistance of the duplex structure to crack initiation and short crack growth.

(iv) The cyclic stress-strain curve and the derived Wöhler curve of high nitrogen SAF 2507 steel are higher than those of SAF 2205 steel while Manson-Coffin curves are identical.

Acknowledgements

This research is part of the research project AV0Z 204 10507. It was supported by the Grant Agency of the Czech Republic, grant No. 106/02/0584 and is gratefully acknowledged.

REFERENCES

[1] NILSON, J. O.: Mater. Sci. Technol., *8*, 1992, p. 687.
[2] www.steel.sandvik.com, www.super-duplex.com
[3] MAGNIN, T.—LARDON, J. —COUDREUSE, I.: In: Low Cycle Fatigue – Directions for the Future. Eds.: Solomon, H. D., Halford, G. R., Kaisand, L. R., Leis, B. N. ASTM STP 942, Philadelphia 1988, p. 43.
[4] DEGALLAIX, S.—SEDDOUKI, A.—NILSON, J. O.—POLÁK, J.: In: High Nitrogen Steels HNS93. Eds.: Gavriljuk, V. G., Nadutov, V. M. Kijev, Int. Metal Physics 1993, p. 420.
[5] VOGT, J. B.—MESSAI, A.—FOCT, J.: In: Proc. Int. Conf. on Duplex Stainless Steels. Ed.: Gooch, T. G. Abington, Woodhead Publishing 1995, paper 33.
[6] MATEO, A.—LLANES, L.—ITURGOYEN, L.—ANGLADA, M.: Acta Mater., *44*, 1996, p. 1143.
[7] NYSTRÖM, M.—KARLSSON, B.: Mater. Sci. Eng., *A215*, 1996, p. 26.
[8] AKDUT, N.: Int. J. Fatigue, *21*, 1999, p. S97.
[9] IACOVIELLO, F.—BONIARDI, M.—LA VECHIA, G. M.: Int. J. Fatigue, *21*, 1999, p. 957.
[10] MATEO, A.—LLANES, L.—AKDUT, N.—ANGLADA, M.: Mater. Sci. Eng., *A319-321*, 2001, p. 516.
[11] POLÁK, J.—ZEZULKA, P.: Fatigue Fracture Engng Mater. Struct. (accepted for publication).